Volume 323, number 3, 267–270 FEBS 12529 June 1993

Non-covalent binding of the heavy atom compound $[Au(CN)_2]^-$ at the halide binding site of haloalkane dehalogenase from *Xanthobacter autotrophicus* GJ10

K.H.G. Verschueren, S.M. Franken*, H.J. Rozeboom, K.H. Kalk and B.W. Dijkstra

BIOSON Research Institute, University of Groningen, Nijenborgh 4, 9747 AG Groningen, The Netherlands

Received 25 March 1993; revised version received 14 April 1993

The $Na[Au(CN)_2]$ heavy atom derivative contributed considerably to the successful elucidation of the crystal structure of haloalkane dehalogenase isolated from *Xanthobacter autotrophicus* GJ10. The gold cyanide was located in an internal cavity of the enzyme, which also contains the catalytic residues. Refinement of the dehalogenase–gold cyanide complex at 0.25 nm to an *R*-factor of 16.7% demonstrates that the heavy atom molecule binds non-covalently between two tryptophan residues pointing into the active site cavity. At this same site also chloride ions can be bound. Therefore, inhibition of dehalogenase activity by the $Au(CN)_2^-$ presumably occurs by competition for the same binding site as substrates.

Protein crystal structure, Dehalogenase; Heavy atom derivative; Gold cyanide; Anion-binding sites in protein

1. INTRODUCTION

Haloalkane dehalogenase from *Xanthobacter autotrophicus* GJ10 converts 1-haloalkanes to their corresponding alcohols and halide ions in a two-step reaction mechanism, via a postulated covalently bound intermediate ester [1–3]. In this reaction no oxygen or cofactors are used, only water is needed as a co-substrate for the hydrolysis of the intermediate ester [3,4] (Fig. 1). Since a broad range of terminally halogenated alkanes are substrates for the enzyme [1], it has a high potential to be applied in the biological degradation of these environmentally toxic compounds [5].

The X-ray structure of haloalkane dehalogenase has been determined by Franken et al. [3] by means of multiple isomorphous replacement (MIR) techniques to solve the phase problem. $Na[Au(CN)_2]$ turned out to provide an excellent single-site heavy atom derivative, which contributed substantially to the successful elucidation of the enzyme's crystal structure [3]. The gold cyanide site appeared to be located in a buried cavity in the interior of the enzyme, which nevertheless must be reachable from the solvent since the heavy atom derivative was soaked into the crystal [3]. This internal cavity, which is predominantly lined with hydrophobic residues, is situated between the two domains of the enzyme. It constitutes the enzyme's active site with residues Asp^{124}, His^{289} and Asp^{260} in a catalytic triad arrangement [3].

As gold cyanide inhibits the dehalogenation reaction in solution, we decided to analyse in detail the binding mode of this compound. Therefore we refined the structure of the dehalogenase–gold cyanide complex at 0.25 nm, and determined the exact interactions of the heavy atom compound with the enzyme. One cyanide moiety is positioned between two tryptophan residues – Trp^{125} and Trp^{175} – in the active site cavity. This same site was also found to bind chloride ions as we could demonstrate from a crystal structure of the dehalogenase complexed with chloride. The other cyanide part might be stabilized by electrostatic interactions with the aromatic ring of Phe^{128}.

Correspondence address: B.W. Dijkstra, Laboratory of Biophysical Chemistry, Department of Chemistry, Nijenborgh 4, 9747 AG Groningen, The Netherlands. Fax: (31) (50) 634800.

**Present address:* Faculty of Chemical Technology, Department of Chemical Physics, University of Twente, P.O. Box 217, 7500 AE Enschede, The Netherlands.

2. MATERIALS AND METHODS

2.1. *Crystal growth and soaking experiments*

Haloalkane dehalogenase purified from *Xanthobacter autotrophicus* GJ10 [1] was crystallized according to Rozeboom et al. [6]. Nicely shaped crystals, suitable for data collection and soaking experiments with heavy atom derivatives, were grown within three weeks by vapor diffusion from a 62% (w/v) saturated (at 0°C) ammonium sulphate solution in a 100 mM bis-Tris-H_2SO_4 buffer of pH 6.2 [6]. The space group of the crystals is $P2_12_12$ with unit cell dimensions of $a = 9.48$ nm, $b = 7.28$ nm and $c = 4.14$ nm, respectively [3,6]. One crystal was soaked at room temperature for one day in a mother liquor solution (62% (w/v) saturated (at 0°C) $(NH_4)_2SO_4$ in 100 mM bis-Tris-H_2SO_4, pH 6.2) containing 3 mM $Na[Au(CN)_2]$ [3]. To analyse chloride binding, a crystal was soaked for one day at room temperature in mother liquor with 10 mM NaCl. Both crystals were isomorphous with the native dehalogenase crystals. The unit cell dimensions of the crystals did not undergo significant changes upon soaking with the different compounds.

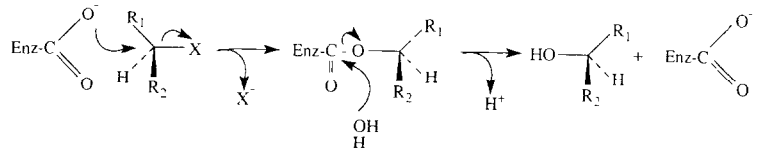

Fig. 1. Proposed reaction mechanism of haloalkane dehalogenase from *Xanthobacter autotrophicus* GJ10 [3].

2.2 *Data collection and processing*

X-ray intensities of the crystallized dehalogenase complexed with the heavy atom derivative were collected at room temperature to a maximum resolution of 0.25 nm on a FAST area detector (Enraf Nonius, Delft, The Netherlands) with graphite monochromatized Cu-K_α radiation from an Elliot GX21 rotating anode [3]. The MADNES package [7] was used for data collection and processing, profile fitting and local scaling of the data set was done according to Kabsch [8], and software from the Groningen BIOMOL crystallographic protein structure determination package was used for merging of the data. A similar data collection set-up was used for the dehalogenase crystal soaked in 10 mM NaCl. More details of the data statistics are summarized in Table I.

2.3. *Refinement*

Independent refinement procedures of the dehalogenase–gold cyanide complex and the dehalogenase–chloride complex were performed with the least-squares reciprocal-space refinement package TNT [9], which was adapted in order to implement the scattering factors of the gold ion [10]. The starting model for both refinements was the native dehalogenase at pH 6.2 refined to 0.19 nm [11] from which all solvent molecules had been deleted. Initial stereochemical geometry for the gold cyanide was generated using standard bond lengths and angles as listed in the 'Tables of Interatomic Distances and Configuration in Molecules and Ions' [12].

Cycles of coordinate and temperature factor refinement were alternated with manual rebuilding on a PS390 Evans and Sutherlands graphics system using the programs FRODO [13] and O [14]. σ_A weighted [15] $(m|F_{obs}| - D|F_{calc}|)\exp(i\alpha_{calc})$ difference maps and $(2m|F_{obs}| - D|F_{calc}|)\exp(i\alpha_{calc})$ electron density maps were calculated in order to include solvent molecules in the model as well as the gold cyanide molecule or the chloride ion, respectively, in the internal cavity of the dehalogenase structure ($|F_{obs}|$(dehalogenase–gold cyanide complex) − $|F_{obs}|$(native)) and ($|F_{obs}|$(dehalogenase–chloride complex) − $|F_{obs}|$(native)). Fouriers were calculated using phases of the 0.19 nm refined native structure [11]. More statistics on the refinement and the geometry of the final dehalogenase–gold cyanide and the dehalogenase–chloride complexes are also listed in Table I.

3. RESULTS AND DISCUSSION

The crystal structure of haloalkane dehalogenase complexed with the heavy atom derivative $[Au(CN)_2]^-$

Table I

Statistics on the data collection and quality of the refined models

	Dehalogenase–gold cyanide pH 6.2	Dehalogenase–chloride pH 6.2
Number of crystals	1	1
Space group	$P2_12_12$	
Unit cell dimensions (nm)	a = 9.48 nm, b = 7.28 nm, c = 4.14 nm	
Resolution range	1.50–0.25 nm	1.50–0.23 nm
Total number of observations	34,819	47,049
Number of unique reflections	9,467	12,008
R_{merge} (%)*	4.88% (on I)	6.09% (on I)
Completeness of the data	88.6% (1.5–0.25 nm)	94.8% (1.5–0.23 nm)
Completeness of the last shell	71.5% (0.258–0.250 nm)	49.8% (0.236–0.234 nm)
Number of residues	1 310	1 310
Number of water molecules	115	180
Number of ligand molecules	1 ($[Au(CN)_2]^-$)	1 (Cl^-)
Overall *B*-factor (nm^2)	0.084 nm^2	0.110 nm^2
Final *R*-factor (%)**	16.7%	16.4%
Estimated coordinate error (determined from a σ_A plot [15])	0.015 nm	0.018 nm
r.m.s. difference for all non-solvent atoms with native dehydrogenase	0.035 nm	0.024 nm
r.m.s. deviations from ideality for:		
covalent bond lengths	0.0013 nm	0.0010 nm
bond angles	3.4°	3.0°

$$*R_{merge}\ (\%) = \frac{\sum_{hkl}\sum_{refl}|I(hkl,j) - \bar{I}(hkl)|}{\sum_{hkl}\sum_{refl}|I(hkl,j)|} \times 100$$

$$**R\text{-factor}\ (\%) = \frac{\sum||F_{obs}| - |F_{calc}||}{\sum|F_{obs}|} \times 100$$

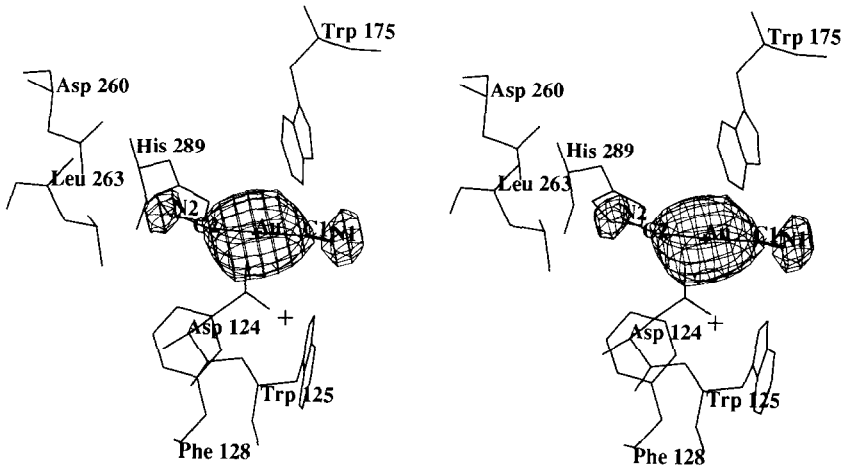

Fig. 2. Stereo view of the σ_A weighted [15] (m $|F_{obs}|$ − D $|F_{calc}|$) exp($i\alpha_{calc}$) electron density of the gold cyanide in the active site cavity of haloalkane dehalogenase contoured at 1.33 σ.

was refined to a final *R*-factor of 16.7% for 9,467 unique reflections between 1.50 and 0.25 nm. The final model contains 115 solvent molecules together with one gold cyanide ion and shows good stereochemical quality as can be seen from Table I. The r.m.s. difference for all non-solvent atoms is 0.035 nm compared to the refined 0.19 nm native dehalogenase structure [11]. The present structure of the dehalogenase–gold cyanide complex clearly demonstrates the binding position of the heavy atom compound in the active site cavity of the dehalogenase. Since gold is a strong atomic scatterer, series termination effects tend to decrease the electron density for the covalent bonds of the gold cyanide compound (Fig. 2). The heavy atom derivative is tightly bound in the internal active site cavity, as is clear from the low average *B*-factors of the atoms of the reagent (Table II). One of the partially negatively charged cyanide moieties of the compound lies on the intersection of the planes of the side-chains of two tryptophan residues pointing into the cavity – Trp^{125} and Trp^{175} – and is stabilized by their slightly positively charged ring nitrogens. We could identify this same site as a halide binding site in the dehalogenase enzyme by soaking experiments with chloride (Table I and II, Fig. 3). The other cyanide part of the reagent is lying in the plane of the aromatic ring of Phe^{128}, interacting with the somewhat positively charged ring hydrogens. Negatively charged groups have been shown before to interact preferentially with the hydrogens in the plane of aromatic rings [16,17], while positively charged groups are attracted more by the π-electron cloud below and above the aromatic rings [18–20]. More details about the geometry of the compound environment and distances are summarized in Table II.

The binding of the large complex $[Au(CN)_2]^-$ anion in the crystal structure of the dehalogenase has caused

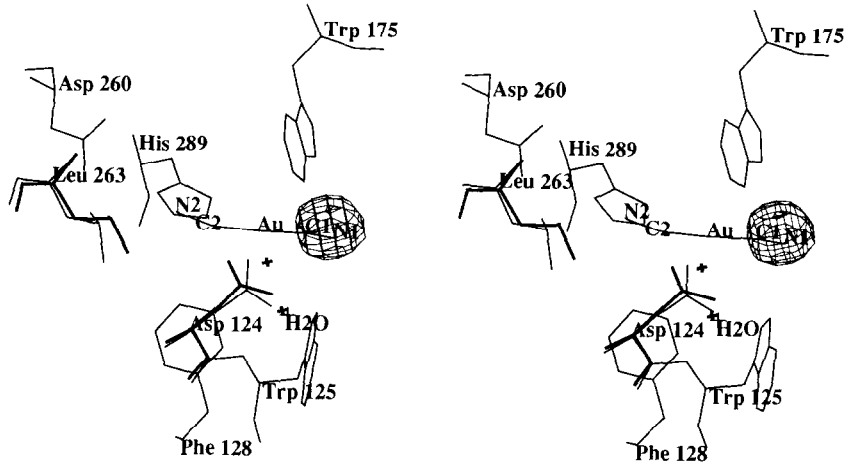

Fig. 3. Stereo view of the active site environment of the dehalogenase–gold cyanide complex (thin lines) superimposed on the native structure of dehalogenase (thick lines), showing the movements of the side-chains of residues Asp^{124} and Leu^{263} upon binding of the gold cyanide molecule. Also shown is the ($|F_{obs}|$(dehalogenase–chloride complex) − ($|F_{obs}|$(native)) electron density of a chloride ion, contoured at 1.33 σ, indicating the position of the halide binding site between the two tryptophan residues.

Table II

Distances of the $[Au(CN)_2]^-$ atoms and the chloride ion to the neighbouring atoms in the active site cavity of the dehalogenase (< 0.40 nm)

	B-factor (nm^2)	Atom	Distance (nm)
A. Dehalogenase–gold cyanide complex			
N_1	0.09	$Trp^{125}N_{\varepsilon 1}$	0.31
		$Trp^{175}N_{\varepsilon 1}$	0.36
		$Phe^{222}O$	0.35
		$Phe^{222}C$	0.34
		$Glu^{56}C_{\beta}$	0.34
C_1	0.05	$Trp^{125}N_{\varepsilon 1}$	0.33
		$Trp^{175}N_{\varepsilon 1}$	0.32
		$Glu^{56}C_{\beta}$	0.37
Au^+	0.08	$Asp^{124}O_{\delta 1}$	0.37
		$Asp^{124}O_{\delta 2}$	0.40
C_2	0.10	$Asp^{124}O_{\delta 1}$	0.37
		$Phe^{128}C_{\zeta}$	0.38
N_2	0.14	$Phe^{128}C_{\zeta}$	0.40
		$Leu^{262}C_{\beta}$	0.38
		$Leu^{263}C_{\gamma}$	0.31
		$His^{289}C_{\varepsilon 1}$	0.34
		$His^{289}C_{\varepsilon 2}$	0.39
B. Dehalogenase–chloride complex			
Cl^-	0.05	$Trp^{125}N_{\varepsilon 1}$	0.34
		$Trp^{175}N_{\varepsilon 1}$	0.32

some local structural rearrangements of a few residues lining the active site cavity, without disrupting the overall structure, however. The side-chains of Asp^{124} – the nucleophile in the reaction mechanism – and Leu^{263} are pushed away, resulting in a slight expansion of the cavity to allow the fit of the gold cyanide (Fig. 3). The displacement of the Asp^{124} side-chain results in the absence of the hydrolytic water molecule, essential for the second step of the reaction mechanism – the hydrolysis of the covalently bound intermediate ester [2,3,11] (Fig. 1). The volume of the cavity containing this water molecule is reduced, allowing space for just one solvent molecule instead of two as has been found in the native dehalogenase structure [11] (Fig. 3), although however, we cannot exclude the possibility of missing electron density for this solvent molecule, due to the limited 0.25 nm resolution reflection data set.

From ^{35}Cl and ^{81}Br nuclear magnetic resonance studies [21] it is known that cyanide compounds can act as competitors towards halogens for high-affinity binding sites in a number of proteins. From the crystal structures of the dehalogenase–gold cyanide and the dehalogenase–chloride complexes, we have shown here that indeed the gold cyanide binds non-covalently with its cyanide part at the halide binding site between the two tryptophan residues – Trp^{125} and Trp^{175} – pointing into the cavity of the dehalogenase. Since modeling studies of 1,2-dichloroethane in the active site cavity indicate that the substrate binds with its chloride ion between the two tryptophan side-chains, gold cyanide most likely acts as an inhibitor of the dehalogenation reaction in solution by binding on the substrate binding site in the active site cavity of the haloalkane dehalogenase.

The structure of the dehalogenase–gold cyanide complex presented here, is a structural confirmation of the findings of Norne et al. [21] that kinetically inert complex anions like $[Au(CN)_2]^-$ and $[Pt(CN)_4]^{2-}$ may bind non-covalently on high-affinity anion-binding sites of proteins. Since such compounds are chemically inert, they also cause less structural modifications in the proteins [21]. Therefore they may provide very useful heavy atom derivatives for the elucidation of crystal structures of proteins [22–24].

Acknowledgements It is a pleasure to thank Dr D B. Janssen and co-workers for their generous supplies of protein material and useful comments, and all members of the Groningen Protein Crystallography Group for their many stimulating discussions.

REFERENCES

[1] Keuning, S., Janssen, D.B. and Witholt, B. (1985) J. Bacteriol. 163, 635–639.
[2] Janssen, D.B., Gerritse, J., Brackman, J., Kalk, C., Jager, D. and Witholt, B. (1988) Eur. J. Biochem. 171, 67–72.
[3] Franken, S.M., Rozeboom, H.J., Kalk, K.H. and Dijkstra, B.W. (1991) EMBO J 10, 1297–1302
[4] Janssen, D B., Pries, F., van der Ploeg, J., Kazemier, B., Terpstra, P. and Witholt, B. (1989) J. Bacteriol. 171, 6791–6799.
[5] Janssen, D.B., Scheper, A., Dijkhuizen, L. and Witholt, B. (1985) Appl. Environm. Microbiol. 49, 673–677.
[6] Rozeboom, H.J., Kingma, J., Janssen, D.B. and Dijkstra, B.W. (1988) J. Mol. Biol. 200, 611–612.
[7] Messerschmidt, A. and Pflugrath, J.W. (1987) J. Appl. Crystallogr. 20, 306–315.
[8] Kabsch, W. (1988) J. Appl. Crystallogr. 21, 916–924.
[9] Tronrud, D.E., ten Eyck, L.F. and Matthews, B.W. (1987) Acta Crystallogr. A43, 489–501
[10] Lee, D.J. (1969) Acta Crystallogr. A25, 712–713.
[11] Verschueren, K H.G., Franken, S.M., Rozeboom, H.J., Kalk, K.H and Dijkstra, B.W., submitted.
[12] Tables of Interatomic Distances and Configuration in Molecules and Ions, supplement, 1956–1959, The Chemical Society, London.
[13] Jones, T.A (1978) J Appl. Crystallogr. 11, 268–272.
[14] Jones, T.A., Zou, J.-Y., Cowan, S.W and Kjeldgaard, M. (1991) Acta Crystallogr. A47, 110–119.
[15] Read, R.J. (1986) Acta Crystallogr. A42, 140–149.
[16] Thomas, K.A., Smith, G M., Thomas, T.B. and Feldman, R.J. (1982) Proc. Natl. Acad Sci. USA 79, 4843–4847.
[17] Reid, K.S.C., Lindley, P.F and Thornton, J M. (1985) FEBS Lett. 190, 209–213.
[18] Tüchsen, E and Woodward, C. (1987) Biochemistry 26, 1918–1925.
[19] Burley, S.K. and Petsko, G.A. (1988) FEBS Lett. 203, 139–143.
[20] Kooystra, P.J.U., Kalk, K H. and Hol, W.G.J (1988) Eur. J. Biochem. 177, 345–349.
[21] Norne, J.-E., Lilja, H., Lindman, B., Einarsson, R. and Zeppezauer, M. (1975) Eur. J. Biochem. 59, 463–473.
[22] Leslie, A.G W (1990) J. Mol. Biol. 213, 167–186.
[23] Knight, S., Andersson, I. and Brändén, C.-I (1990) J. Mol. Biol 215, 113–160.
[24] Herzberg, O. (1991) J. Mol. Biol. 217, 701–719.